

1       Lysophosphatidylcholine acyltransferase 3 is decreased in  
2           non-alcoholic steatohepatitis, resulting in caspase-  
3           independent hepatocyte death

4  
5                           Keisuke Kakisaka <sup>1</sup>  
6                           Yuji Suzuki <sup>1</sup>  
7                           Yudai Fujiwara <sup>1</sup>  
8                           Akiko Suzuki <sup>1</sup>  
9                           Jo Kanazawa <sup>1</sup>  
10                          Yasuhiro Takikawa <sup>1</sup>

11  
12       1) Division of Hepatology, Department of Internal medicine, School of  
13           medicine, Iwate Medical University, Morioka, Japan

14  
15   Key words: lysophosphatidylcholine, RIP1, ER stress, JNK, NAFLD, NASH,  
16   palmitate

17  
18  
19   Address for correspondence: Keisuke Kakisaka, M. D., Ph. D.  
20                               School of Medicine  
21                               Iwate Medical University  
22                               19-1 Uchimaru Morioka  
23                               Iwate, Japan 0208505  
24                               Tel. : +81-19-651-5111  
25                               Fax: +81-19-652-6664  
26                               E-mail: keikaki@iwate-med. ac. jp

27  
28  
29   Running title: Lysophosphatidylcholine acyltransferase 3 in lipotoxicity

30  
31   Number of:  
32       Figures 4  
33       Supplemental figures 2  
34       Supplemental material and method 1  
35       References 25

36  
37   Abbreviations: BEL, bromoenol lactone; DAG, diacylglycerol; ER,  
38   endoplasmic reticulum; FFA, free fatty acids; GSK-3, glycogen synthase  
39   kinase-3; HPH, human primary hepatocytes; JNK, c-Jun N-terminal kinase;  
40   LPC, lysophosphatidylcholine; lysophosphatidylcholine acyltransferase,

41 LPCAT; NAFLD, nonalcoholic fatty liver disease; NASH, nonalcoholic  
42 steatohepatitis; PACOCF<sub>3</sub>, palmityl trifluoromethyl ketone; PC,  
43 phosphatidylcholine; PLA2, phospholipase A2; RIP, receptor-interacting  
44 protein kinases

1 **Background & Aims:** Lipotoxicity causes liver inflammation, which leads to  
2 non-alcoholic steatohepatitis (NASH). Lysophosphatidylcholine (LPC) is a  
3 causal agent of lipotoxicity. Recently, lysophosphatidylcholine  
4 acyltransferase (LPCAT) was identified as an enzyme that catalyzes the  
5 esterification of LPC, which potentially decreases LPC levels. However, the  
6 effect of LPCAT in lipotoxicity of the liver is not fully understood. Our aim  
7 was to determine whether LPCAT attenuates lipotoxicity in the liver. **Methods:**  
8 Mice fed a high-fat diet with/without sucrose (HFDS/HFD) and Huh-7 cells  
9 treated with palmitate were used. **Results:** Mice fed HFDS showed advanced  
10 liver fibrosis as compared to mice fed HFD or normal chow. LPCAT3 mRNA  
11 expression in the liver was significantly decreased in the HFDS liver, and LPC  
12 content in the HFDS liver was significantly increased as compared to the other  
13 groups. When Huh-7 cells with shRNA-mediated knockdown of LPCAT3 (shLPCAT3  
14 cells) were treated with palmitate, the intracellular LPC concentration and  
15 cell death were significantly higher than those in wild-type Huh-7 cells.  
16 Palmitate-induced cell death in shLPCAT3 was attenuated by a combination of  
17 receptor-interactive protein kinase 1 inhibitor with pan-caspase inhibitor. In  
18 contrast, intracellular LPC and palmitate-induced cell death were  
19 significantly lower in LPCAT3-overexpressing Huh-7 cells than in wild-type  
20 cells. **Conclusion:** Depletion of LPCAT3 in a mouse model of NASH leads to

1 caspase-independent cell death, and LPCAT3 is a potential therapeutic target  
2 in NASH.  
3

## 1 Introduction

2 Non-alcoholic fatty liver disease (NAFLD), which is a manifestation of  
3 the metabolic syndrome in the liver, is highly prevalent in western countries.  
4 Non-alcoholic steatohepatitis (NASH) is a subset of NAFLD that is accompanied  
5 by inflammation and may lead to cirrhosis <sup>1, 2</sup>. Serum free fatty acids (FFA)  
6 are higher in patients with NASH than in healthy subjects <sup>3</sup>. Furthermore,  
7 saturated FFA, such as palmitate (PA) can induce apoptosis in hepatocytes <sup>4-7</sup>.  
8 Thus, toxic lipids, such as saturated FFA, are one of the suspected causes of  
9 NASH.

10 Lysophosphatidylcholine (LPC), a metabolite of FFA, is a major  
11 phospholipid generated from phosphatidylcholine (PC) by phospholipase A2  
12 (PLA2) <sup>8</sup>. Inhibition of PLA2 decreases the concentration of LPC in hepatocytes  
13 and attenuates FFA-induced lipoapoptosis <sup>9</sup>. In a rat model of NAFLD, serum  
14 alanine aminotransferase (ALT) levels were increased in correlation with serum  
15 LPC levels <sup>10</sup>. LPC directly induces apoptosis via a pathway that is largely  
16 indistinguishable from saturated FFA-induced lipoapoptosis <sup>9, 11</sup>. Therefore, LPC  
17 is considered as a casual substrate for lipotoxicity in the liver.

18 Shindou et al. identified lysophosphatidylcholine acyltransferase  
19 (LPCAT) as an enzyme that catalyzes the esterification of LPC <sup>12</sup>. LPCAT  
20 regulates cell-membrane glycerolipid remodeling in the so-called “Lands  
21 cycle.” LPCAT is classified into four subtypes, LPCAT1-4, on the basis of the

1 phospholipid substrate <sup>12</sup>. According to its enzymatic activity, LPCAT can  
2 decrease FFA-induced LPC generation. However, the influence of LPCAT in  
3 lipoapoptosis remains unclear.

4       The present study aimed to investigate whether and how LPCAT affects  
5 lipotoxicity in the liver. To this end, we employed a NASH mouse model for *in-*  
6 *vivo* study and a hepatoma cell line (Huh-7) for *in-vitro* study.

7

1     **EXPERIMENTAL PROCEDURES**

2             *Animals.* Male 4-week-old C57BL/6J mice were obtained from Charles River  
3 Laboratories (Charles River, Yokohama, Japan) and were maintained on a 12-h  
4 light/12-dark cycle in humidity-controlled rooms at 22 ° C with *ad libitum*  
5 access to drinking water. After 1 week of habituation, 10 mice each were  
6 assigned to normal chow (Cont), high-fat diet (HFD-60; Oriental Yeast Co.,  
7 Tokyo, Japan) alone (HFD), and HFD with sucrose supplementation (42 g/L)  
8 groups (HFDS) and were fed their respective diets for 16 weeks. Three mice of  
9 each group were examined by intraperitoneal glucose tolerant test (IPGTT). The  
10 remaining seven mice of each group were sacrificed using isoflurane anesthesia  
11 after overnight fasting at 21 weeks of age. Three of the seven mice of each  
12 group were analyzed for liver LPC content. All of the animal experiments were  
13 approved by the Animal Care and Use Committee of Iwate Medical University  
14 (Morioka, Japan; 28-001). Liver samples were subjected hematoxylin-eosin  
15 staining for steatosis and Masson-Goldner staining for fibrosis for  
16 histological evaluation. Serum aspartate aminotransferase (AST) and total  
17 cholesterol (TC) were measured with an autoanalyzer (JCA-BM2250; JEOL, Tokyo,  
18 Japan).

19             *Cells.* Huh-7 cells, a human hepatocellular carcinoma cell line, were  
20 maintained in Dulbecco' s modified Eagle' s medium containing glucose (25 mM)  
21 supplemented with 10% fetal bovine serum, 100,000 IU/L penicillin, and 100

1 mg/L streptomycin. In addition, we employed Huh-7 cells that stably expressed  
2 a short-hairpin RNA (shRNA) complementary to LPCAT3 (shLPCAT3 cells) and  
3 LPCAT3 overexpression (LPCAT3 OE) cells generated from Huh-7 cells by using  
4 lentivirus vector (RC209485L2; OriGene, Rockville, MD). The cells were treated  
5 with palmitate (PA) (#P5585; Sigma-Aldrich, St. Louis, MO). PA was dissolved  
6 in isopropanol at a stock concentration of 160 mM. The final concentration of  
7 PA was  $\leq 0.2\%$  in the medium, and the corresponding isopropanol concentration  
8 was used as a vehicle control (Veh).

9 *Measurement of the phospholipid concentration in cells or the liver.*

10 Cellular LPC in *in-vitro* experiments was measured by an enzymatic assay as  
11 reported by Kishimoto et al.<sup>13</sup>. We previously reported details on this assay  
12 for *in-vitro* setting<sup>9</sup>.

13 Total lipids of the liver were extracted by the method of Bligh and Dyer  
14<sup>14</sup>. Phospholipids were separated from total lipids using a diethylaminoethyl-  
15 cellulose column. Liquid chromatography-electrospray ionization-tandem mass  
16 spectrometry was carried out using a TSQ-Vantage (Thermo Fisher Scientific,  
17 Waltham, MA, USA) with an UltiMate 3000 LC system (Thermo Fisher Scientific)  
18 equipped with an HTC PAL autosampler (CTC Analytics, Zwingen, Switzerland).  
19 LPC and PC were measured by selected reaction monitoring in the negative ion  
20 mode.

1            *Statistical analysis.* All data represent at least three independent  
2 experiments and are expressed as the mean  $\pm$  SD. Differences between groups  
3 were compared using Student' s *t*-test and one-way analysis of variance with a  
4 *post-hoc* Dunnett test. Significance was accepted at  $p < 0.05$ .

5            Materials and methods for intraperitoneal glucose tolerant test,  
6 quantitation of cell death, quantitative real-time PCR, immunoblot analysis,  
7 XBP1 splicing analysis, and antibodies and reagents are provided in the  
8 Supplementary Information.

9

1 RESULTS

2 *HFD induces fatty liver and insulin resistance in mice, and sucrose*  
3 *supplementation enhances HFD-induced inflammation and fibrosis in the liver*

4 To confirm the effect of HFD and sucrose supplementation in mice, we  
5 evaluated histological findings of the liver and laboratory data, and we  
6 monitored body weight. Body weight was significantly higher in HFD and HFDS  
7 than in Cont animals (Figure 1A). AST and TC were significantly higher in HFD  
8 and HFDS than in Cont (Figure 1B and 1C). Furthermore, HFD and HFDS showed  
9 prolonged glucose elevation after intraperitoneal administration of glucose  
10 (Figure 1D). In histological evaluation, HFD and HFDS revealed overt lipid  
11 accumulation in the liver (Figure 1E). Furthermore, pericellular fibrosis and  
12 lymphocyte accumulation were observed in the HFDS liver (Figure 1E). mRNA  
13 expression of alpha smooth muscle actin and collagen I and collagen III was  
14 significantly higher in the HFDS than in the HFD and Cont livers (Supplemental  
15 Figure 1A-C). These data revealed that HFDS in the present study induced  
16 steatohepatitis with insulin resistance in mice, which were therefore  
17 considered a NASH model. Since LPC is considered as a causal substance for  
18 liver injury thorough hepatocyte apoptosis, we evaluated the LPC content in  
19 the liver in each group. The liver LPC concentration was significantly higher  
20 in HFDS than in HFD and Cont (Figure 1F). In addition, the level of PC, a

1 source of LPC, was also elevated in HFDS and HFD compared to Cont  
2 animals (Figure 1F).

3 *LPCAT3 expression is decreased in mice fed HFDS*

4 As the LPC content in the liver of NASH mice was increased (Figure 1F),  
5 we reasoned that LPCAT family activity would be altered in these mice.  
6 Therefore, we evaluated the expression of LPCATs in the liver among Cont, HFD,  
7 and HFDS animals (Figure 1G). Although the expression of LPCAT1 and LPCAT2  
8 tended to be decreased in HFD and HFDS as compared to Cont, the difference was  
9 not significant. In contrast, LPCAT3 expression was significantly lower in the  
10 HFDS liver than in the Cont and the HFD liver. LPCAT4 expression was lower in  
11 the HFDS liver than in the Cont, but not the HFD liver. On the basis of these  
12 data, we hypothesized that the decrease in LPCAT3 expression was associated  
13 with NASH progression. Therefore, we focused on the effect of LPCAT3 in  
14 lipotoxicity.

15 *Knockdown of LPCAT3 increases PA-induced cell death, which is mediated*  
16 *by LPC*

17 To evaluate the influence of LPCAT3 in lipotoxicity, we used PA, which  
18 is known as a toxic lipid. By using shRNA-mediated RNA interference, we  
19 knocked down LPCAT3 expression in Huh7 cells (Supplemental Figure 2A). As  
20 anticipated, PA cytotoxicity was enhanced in shLPCAT3 as compared to wild-type  
21 (WT) Huh7 cells as indicated by a biochemical assay (Figure 2A) and

1 morphological assessment (Figure 2B). To investigate whether PA-induced cell  
2 death in shLPCAT3 was mediated by the generation of LPC, we used  
3 pharmacological phospholipase A2 inhibitors, bromo-enol lactone and palmityl  
4 trifluoromethyl ketone. The two inhibitors significantly reduced PA-induced  
5 cell death in shLPCAT3 cells as well as the PA-induced increase LPC content  
6 (Figure 2C-E). These data indicated that the enhanced cytotoxicity of PA in  
7 shLPCAT3 was mediated by an increase in the LPC level due to knockdown of  
8 LPCAT3.

9 *Endoplasmic reticulum stress and JNK phosphorylation do not show*  
10 *significant differences between shLPCAT3 and WT during lipotoxic insult*

11 We next evaluated in detail how lipotoxicity in shLPCAT3 cells induced  
12 cell death. To this end, we evaluated several signaling molecules that were  
13 previously reported as key signals during lipoapoptosis<sup>3, 15, 16</sup>. JNK  
14 phosphorylation and the ER stress response, assessed as eIF2a phosphorylation  
15 and XBP1 splicing, respectively, were increased by incubation with PA in both  
16 WT and shLPCAT3 cells; however, all these signals did not show a significant  
17 difference between the WT and shLPCAT3 cells (Figure 2F and 2G).

18 *PA-induced cell death in shLPCAT3 cells is mediated by both caspase-*  
19 *dependent and -independent mechanisms*

20 Because PA-induced cell death was considered as caspase-dependent  
21 apoptosis, we checked whether the pan-caspase inhibitor QVD-OPh was able to

1 prevent PA-induced cell death in shLPCAT3s. While QVD-OPh prevented PA-induced  
2 cell death in both WT and shLPCAT3 cells, its effect in shLPCAT3 cells was  
3 lower than that in WT cells (Figure 3A and 3B). We next evaluated the effect  
4 of the RIPK1 inhibitor necrostatin because necroptosis was suggested as  
5 another cause of hepatocyte death in NASH<sup>17-19</sup>, and RIPK1 is known as a key  
6 molecule in necroptosis. The combination of necrostatin and QVD-OPh  
7 significantly reduced PA-induced cell death in shLPCAT3 cells (Figure 3A and  
8 3B).

9 *LPCAT3 overexpression decreases PA-induced CHOP expression and reduces*  
10 *PA-induced cell death*

11 To confirm the protective effect of LPCAT3 during lipotoxicity, we  
12 generated LPCAT3-overexpressing Huh7 cells (LPCAT3OE). Overexpression of  
13 LPCAT3 was confirmed at the mRNA level, and clones 1 and 2 significantly  
14 overexpressed LPCAT3 when compared with WT cells (Supplemental Figure 2B). PA-  
15 induced expression of CHOP, which is a transcriptional factor that serves as  
16 an ER stress marker, was significantly decreased in LPCAT3OE cells (Figure 4A).  
17 Moreover, phosphorylation of eIF2 and PA-induced cell death were significantly  
18 decreased in LPCAT3OE compared to WT cells (Figure 4B). Finally, the PA-  
19 induced increase in intracellular LPC was significantly attenuated in LPCAT3OE  
20 as compared to WT cells (Figure 4C).

21

## 1 DISCUSSION

2 NASH is expected to become a primary indication for liver  
3 transplantation due to hepatocellular carcinoma, liver cirrhosis, and liver  
4 failure <sup>20, 21</sup>. Because inflammation due to hepatocyte death promotes fibrosis  
5 in the NASH liver, lipotoxicity-induced hepatocyte death needs to be  
6 eliminated. To aid in the establishment of therapeutic targets on the basis of  
7 the pathophysiology of lipotoxicity-induced hepatocyte death, we investigated  
8 the effect of LPCAT3 during lipotoxicity in the liver. The present study  
9 revealed that (1) LPCAT3 expression in the liver was decreased in a HDF-  
10 induced mouse model of NASH, (2) depletion of LPCAT3 enhanced PA-induced  
11 hepatocyte death, (3) PA-induced cell death under LPCAT3 depletion was  
12 executed by caspase-independent machinery, and (4) LPCAT3 overexpression  
13 decreased PA-induced CHOP expression and attenuated PA-induced cell death.  
14 These results indicate that LPCAT3 might serve as a therapeutic target in NASH  
15 through a decrease in hepatocyte death.

16 In the present study, LPC was elevated and LPCAT3 expression was  
17 downregulated in the livers of NASH model mice. In an *in-vitro* study, the PA-  
18 induced increase in intracellular LPC and, accordingly, in hepatocyte death,  
19 was enhanced in LPCAT3 knockdown- and attenuated in LPCAT3-overexpressing  
20 cells. These data indicated that LPCAT3 protected against lipotoxicity and  
21 that depletion of LPCAT3 might be associated with the pathophysiology of NASH.

1 However, how LPCAT3 is suppressed in mice on HFDS remains uncertain. We  
2 speculated that a disturbance of the phospholipid metabolism might affect  
3 LPCAT3 expression. In NASH patients, PC levels in both the liver and the  
4 plasma are significantly higher than those in healthy subjects. Similarly,  
5 this study showed that PC levels in both HFD and HFDS mice were higher than  
6 those in control group (Figure 1F). In addition, phospholipase A2 inhibitor  
7 decreased the PA-induced LPC elevation (Figure 2E). Thus, PC levels in NASH  
8 are high, although PC is normally converted to LPC by phospholipase A2. LPCAT3,  
9 as a reverse pathway, converts PC to LPC. Thus, we hypothesize that the excess  
10 PC might suppress the LPCAT3 pathway. However, LPCAT3 has enzymatic activity  
11 toward other phospholipids, such as phosphatidylserine and  
12 phosphatidylethanolamine, and thus, these phospholipids might affect LPCAT3  
13 expression, although the association between these phospholipids and LPCAT3  
14 expression in this study remains unclear. **Thus, our hypothesis requires further study.**

15 RIPKs, which constitute a family of seven members, are crucial  
16 regulators of cell survival and death. Interaction between RIPK1 and RIPK3 is  
17 important for necroptosis<sup>22</sup>. Necroptosis occurs when caspase 8 is inactivated  
18 on the extrinsic cell death pathway. During necroptosis, RIPK1 and RIPK3 form  
19 a complex that is involved in organelle swelling and rupture<sup>22</sup>. As a result,  
20 necroptosis promotes inflammation by regulating the release of intracellular  
21 damaged-associated molecular patterns<sup>23, 24</sup>. A previous study showed that a

1 RIPK1 inhibitor attenuated inflammation of the NASH liver *in vivo*<sup>19</sup>. Thus,  
2 necroptosis was reasoned to be one of the causes of hepatocyte death in NASH  
3<sup>19</sup>. However, how necroptosis was induced in the NASH liver remained unclear.  
4 Obviously, the caspase-dependent pathway of lipoapoptosis is the main form of  
5 hepatocyte death in the NASH liver<sup>25</sup>. However, lipid-induced cell death in  
6 LPCAT3-depleted hepatocytes was considered as necroptosis because it was  
7 attenuated by a combination of pan-caspase inhibitor and RIPK1 inhibitor.  
8 Because hepatocyte death in this study was associated with caspase-dependent  
9 as well as -independent pathways, LPCAT3-depleted hepatocytes showed lipid-  
10 induced cell death heterogeneity. The present study newly suggests that  
11 impaired phospholipid metabolism induces necroptosis upon abundant execution  
12 of apoptosis due to lipotoxic insult.

13 We recognize several limitations of the present study. First, the  
14 functions of other LPCATs remain unclear. The expression of all LPCATs tended  
15 to decrease in the HFD as well as the HFDS liver, although these changes were  
16 not significant. We did not exclude whether or not these changes would be  
17 compensative. In the present study, we only demonstrated that LPCAT3 might be  
18 a potential therapeutic target of NASH. Second, heterogeneous cell death was  
19 not elucidated in the mouse model. Since the *in-vivo* experiment in the present  
20 study was an observational study based on histological findings, two major  
21 types of cell death, apoptosis and necroptosis, were not distinguishable.

1 Third, LPCAT3 expression in the NASH liver was not confirmed. We assessed mRNA  
2 LPCAT3 expression in the liver by qRT-PCR; however, an antibody to detect the  
3 protein is currently not available. Finally, the mechanism of necroptosis in  
4 LPCAT3-depleted hepatocytes remains unclear. Although LPCAT3 depletion may  
5 lead to two types of cell death during lipotoxic insults, there was no  
6 significant difference in endoplasmic reticulum stress and JNK phosphorylation  
7 between WT and shLPCAT3 cells. Thus, how the disturbance of lipid metabolism  
8 due to LPCAT3 depletion induces the two types of cell death is not fully  
9 understood.

10 In conclusion, the present study led to the following significant  
11 findings: LPCAT3 is depleted in the NASH mouse model and leads to caspase-  
12 dependent/-independent cell death, and LPCAT3 attenuates lipotoxicity by  
13 decreasing the intracellular LPC content. Based on these findings, we conclude  
14 that LPCAT3 is a potential therapeutic target for NASH. Further study on the  
15 detailed characteristics of LPCAT3-overexpressing hepatocytes is needed  
16 because LPCAT3 will affect phospholipid metabolism and cellular membrane  
17 homeostasis.

1           **ACKNOWLEDGEMENTS**

2           This work was supported by KAKENHI Grant Number JP18K07980 (to K.K.) and  
3           TaNeDS grant program from Daiichi Sankyo Co., Ltd. (to K.K.). We thank Gregory  
4           J. Gores for mentorship, Steve F. Bronk for generation of LPCAT3 knockdown  
5           Huh-7 cells, Hiroki Nakanishi (Akita Lipid Technology) for measurement of  
6           phospholipids in the liver.

7

8           **CONFLICTS OF INTEREST**

9           The authors declare that they do not have conflict of interest with  
10          respect to this manuscript.

11

1 FIGURE LEGENDS

2           Figure 1. Mice fed high-fat diet with/without sucrose show overweight,  
3 impaired glucose tolerance, high liver enzyme content, and hypercholesteremia,  
4 and HFDS induces inflammation and fibrosis in the liver and decreases liver  
5 LPCAT3 mRNA expression. *A*, Time course of changes in body weight for mice  
6 fed normal chow (Cont), high-fat diet (HFD) and high fat diet with sucrose  
7 (HFDS). *B* and *C*, Serum aspartate aminotransferase (AST; *B*) and total  
8 cholesterol (TC; *C*) levels at 16 weeks of feeding. The serum concentration of  
9 the indicated parameter is shown on the vertical axis, treatment groups on the  
10 horizontal axis. *D*, Intraperitoneal glucose tolerance test (IPGTT) results.  
11 Each mouse received 2 g/kg of glucose intraperitoneally. The plasma glucose  
12 concentration and time points after glucose administration are indicated on  
13 the vertical and the horizontal axis, respectively. *E*, Representative  
14 microscopic images of liver sections subjected to hematoxylin and eosin  
15 staining (upper panels, magnification, 50 × ) and Masson' s trichrome staining  
16 (lower panels, magnification, 50×) for histological evaluation. *F*,  
17 Lysophosphatidylcholine (LPC) and phosphatidylcholine (PC) levels of the liver  
18 were measured by liquid chromatography-electrospray ionization-tandem mass  
19 spectrometry. *G*, mRNA expression of the indicated genes as analyzed by qRT-  
20 PCR. Gene expression relative to that of GAPDH is indicated on the vertical

1 axis, treatment groups on the horizontal axis. Data are the mean  $\pm$  SD from  
2 seven experiments; \* $P$ <0.05.

3 **Figure 2. LPCAT3 knockdown enhances lipotoxicity by increasing LPC**  
4 **production in hepatocytes, but lipotoxicity is not enhanced by JNK, eIF2a,**  
5 **and endoplasmic reticulum stress.** *A* and *B*, Wild-type Huh-7 cells (WT) and  
6 LPCAT3 knockdown Huh-7 cells (shLPCAT3) were incubated with palmitate (PA; 800  
7  $\mu$ M) for 6 h. Vehicle-treated cells (Veh) were used as controls. Caspase 3/7  
8 catalytic activity was assessed by a fluorogenic assay and expressed as fold  
9 change (*A*). Cell death was assessed by fluorescence positivity after propionic  
10 iodine staining (*B*). *C* and *D*, Huh-7 cells were incubated with PA (800  $\mu$ M) in  
11 the presence of a phospholipase A2 inhibitors (20  $\mu$ M bromoenol lactone [BEL]  
12 and 60  $\mu$ M palmityl trifluoromethyl ketone [PACOCF3]) for 6 h. Caspase 3/7  
13 catalytic activity was assessed by a fluorogenic assay and expressed as fold  
14 change (*C*). Cell death was assessed by fluorescence positivity after propionic  
15 iodine staining (*D*). *E*, Intracellular lysophosphatidylcholine (LPC) levels  
16 were measured by an enzyme-linked colorimetric assay. PA induced an increase  
17 in LPC above basal levels. WT and shLPCAT3 cells were treated with PA at 400  
18 or 800  $\mu$ M for 6 h. These cells were also incubated with/without 20  $\mu$ M BEL and  
19 60  $\mu$ M PACOCF3 for 6 h. *F*, Immunoblot analysis of phosphorylated JNK, total  
20 JNK, phosphorylated eIF2a and total eIF2a. Whole cell lysates were prepared  
21 from WT cells and clones 1 and 2 of shLPCAT3 cells. The cells were incubated

1 with PA (800  $\mu$ M) for 6 h. The data (phosphorylated-to-total JNK ratio) for  
2 each treatment as normalized to it's own Veh control was shown in the lower  
3 graph. *G*: WT and shLPCAT3 cells were treated with either Veh or 800  $\mu$ M PA for  
4 6 h. XBP-1 cDNA was amplified by PCR followed by 1 h incubation with *Pst*I.  
5 Unspliced and spliced forms are presented. Data are the mean  $\pm$  SD from four  
6 experiments; \* $P$ <0.05.

7 **Figure 3. PA-induced cell death in LPCAT3 knockdown Huh-7 cells is**  
8 **ameliorated by a combination of pan-caspase inhibitor and RIPK1 inhibitor.** *A*  
9 and *B*, Huh-7 cells (WT) and LPCAT3 knockdown Huh-7 cells (shLPCAT3) were  
10 incubated with PA (800  $\mu$ M) in the presence of QVD-OPh (20  $\mu$ M) alone,  
11 necrostatine (100  $\mu$ M) alone or combination of these agents for 6 h. Cells  
12 treated with vehicle (Veh) were used as controls. Caspase 3/7 catalytic  
13 activity was assessed by a fluorogenic assay and expressed as fold change (*A*).  
14 Cell death was assessed by fluorescence positivity after propionic iodine  
15 staining (*B*). Data are the mean  $\pm$  SD from four experiments; \* $P$ <0.05.

16

17

18 **Figure 4. LPCAT3 overexpression ameliorates PA-induced cell death by**  
19 **suppressing the increase in intracellular LPC and CHOP expression.** *A*, *B* and *C*,  
20 Huh-7 cells (WT) and LPCAT3-overexpressing Huh-7 cells (LPCAT3OE) were  
21 incubated with PA (800  $\mu$ M) for the indicated time. Vehicle (Veh)-treated

1 cells were used as controls. Immunoblot analysis of CHOP. Whole cell lysates  
2 were prepared from WT cells and clones 1 and 2 of LPCAT30E cells. The cells  
3 were incubated with PA (800  $\mu$ M) for 16 h (*A*). Cell death was assessed by  
4 fluorescence positivity after propionic iodine staining. WT and LPCAT30E cells  
5 were treated with PA for 16 h (*B*). Intracellular LPC levels were measured by  
6 an enzyme-linked colorimetric assay. PA induced an increase in LPC above basal  
7 levels in WT cells treated with Veh. WT and LPCAT30E cells were treated with  
8 PA for 8 h (*C*). All data in (B) and (C) are expressed as the mean  $\pm$  SD from  
9 three experiments;  $*P < 0.05$ .

## 1 REFERENCES

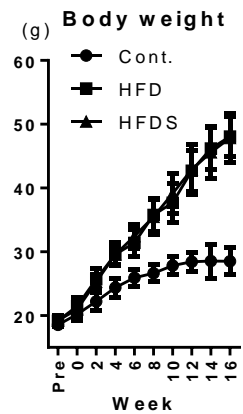
- 2 [1] Adams LA, Lymp JF, St Sauver J, *et al.* The natural history of nonalcoholic fatty  
3 liver disease: a population-based cohort study. *Gastroenterology*. 2005; **129**: 113-21.
- 4 [2] Ekstedt M, Franzen LE, Mathiesen UL, *et al.* Long-term follow-up of patients  
5 with NAFLD and elevated liver enzymes. *Hepatology*. 2006; **44**: 865-73.
- 6 [3] Ibrahim SH, Kohli R, Gores GJ. Mechanisms of lipotoxicity in NAFLD and  
7 clinical implications. *J Pediatr Gastroenterol Nutr*. 2011; **53**: 131-40.
- 8 [4] Akazawa Y, Cazanave S, Mott JL, *et al.* Palmitoleate attenuates palmitate-induced  
9 Bim and PUMA up-regulation and hepatocyte lipoapoptosis. *J Hepatol*. 2010; **52**: 586-93.
- 10 [5] Masuoka HC, Mott J, Bronk SF, *et al.* Mcl-1 degradation during hepatocyte  
11 lipoapoptosis. *J Biol Chem*. 2009; **284**: 30039-48.
- 12 [6] Han MS, Park SY, Shinzawa K, *et al.* Lysophosphatidylcholine as a death effector  
13 in the lipoapoptosis of hepatocytes. *J Lipid Res*. 2008; **49**: 84-97.
- 14 [7] Singh R, Wang Y, Xiang Y, Tanaka KE, Gaarde WA, Czaja MJ. Differential effects  
15 of JNK1 and JNK2 inhibition on murine steatohepatitis and insulin resistance.  
16 *Hepatology*. 2009; **49**: 87-96.
- 17 [8] Fu S, Yang L, Li P, *et al.* Aberrant lipid metabolism disrupts calcium homeostasis  
18 causing liver endoplasmic reticulum stress in obesity. *Nature*. 2011; **473**: 528-31.
- 19 [9] Kakisaka K, Cazanave SC, Fingas CD, *et al.* Mechanisms of  
20 lysophosphatidylcholine-induced hepatocyte lipoapoptosis. *Am J Physiol Gastrointest*  
21 *Liver Physiol*. 2012; **302**: G77-84.
- 22 [10] Huang Y, Fu JF, Shi HB, Liu LR. [Metformin prevents non-alcoholic fatty liver  
23 disease in rats: role of phospholipase A2/lysophosphatidylcholine lipoapoptosis  
24 pathway in hepatocytes]. *Zhonghua Er Ke Za Zhi*. 2011; **49**: 139-45.
- 25 [11] Kakisaka K, Cazanave SC, Werneburg NW, *et al.* A hedgehog survival pathway  
26 in 'undead' lipotoxic hepatocytes. *J Hepatol*. 2012; **57**: 844-51.
- 27 [12] Shindou H, Hishikawa D, Harayama T, Yuki K, Shimizu T. Recent progress on  
28 acyl CoA: lysophospholipid acyltransferase research. *J Lipid Res*. 2009; **50 Suppl**: S46-51.
- 29 [13] Kishimoto T, Soda Y, Matsuyama Y, Mizuno K. An enzymatic assay for  
30 lysophosphatidylcholine concentration in human serum and plasma. *Clin Biochem*. 2002;  
31 **35**: 411-6.
- 32 [14] Bligh EG, Dyer WJ. A rapid method of total lipid extraction and purification. *Can*  
33 *J Biochem Physiol*. 1959; **37**: 911-7.
- 34 [15] Akazawa Y, Nakao K. To die or not to die: death signaling in nonalcoholic fatty  
35 liver disease. *J Gastroenterol*. 2018; **53**: 893-906.
- 36 [16] Akazawa Y, Nakao K. Lipotoxicity pathways intersect in hepatocytes:  
37 Endoplasmic reticulum stress, c-Jun N-terminal kinase-1, and death receptors. *Hepatol*  
38 *Res*. 2016; **46**: 977-84.

- 1 [17] Roychowdhury S, McCullough RL, Sanz-Garcia C, *et al.* Receptor interacting  
2 protein 3 protects mice from high-fat diet-induced liver injury. *Hepatology*. 2016; **64**:  
3 1518-33.
- 4 [18] Afonso MB, Rodrigues PM, Carvalho T, *et al.* Necroptosis is a key pathogenic  
5 event in human and experimental murine models of non-alcoholic steatohepatitis. *Clin*  
6 *Sci (Lond)*. 2015; **129**: 721-39.
- 7 [19] Gautheron J, Vucur M, Reisinger F, *et al.* A positive feedback loop between RIP3  
8 and JNK controls non-alcoholic steatohepatitis. *EMBO Mol Med*. 2014; **6**: 1062-74.
- 9 [20] Kabbany MN, Conjeevaram Selvakumar PK, Watt K, *et al.* Prevalence of  
10 Nonalcoholic Steatohepatitis-Associated Cirrhosis in the United States: An Analysis of  
11 National Health and Nutrition Examination Survey Data. *Am J Gastroenterol*. 2017; **112**:  
12 581-7.
- 13 [21] Estes C, Razavi H, Loomba R, Younossi Z, Sanyal AJ. Modeling the epidemic of  
14 nonalcoholic fatty liver disease demonstrates an exponential increase in burden of  
15 disease. *Hepatology*. 2018; **67**: 123-33.
- 16 [22] Jouan-Lanhouet S, Arshad MI, Piquet-Pellorce C, *et al.* TRAIL induces necroptosis  
17 involving RIPK1/RIPK3-dependent PARP-1 activation. *Cell Death Differ*. 2012; **19**: 2003-  
18 14.
- 19 [23] Murakami Y, Matsumoto H, Roh M, *et al.* Programmed necrosis, not apoptosis, is  
20 a key mediator of cell loss and DAMP-mediated inflammation in dsRNA-induced  
21 retinal degeneration. *Cell Death Differ*. 2014; **21**: 270-7.
- 22 [24] Vanden Berghe T, Vanlangenakker N, Parthoens E, *et al.* Necroptosis, necrosis  
23 and secondary necrosis converge on similar cellular disintegration features. *Cell Death*  
24 *Differ*. 2010; **17**: 922-30.
- 25 [25] Malhi H, Bronk SF, Werneburg NW, Gores GJ. Free fatty acids induce JNK-  
26 dependent hepatocyte lipoapoptosis. *J Biol Chem*. 2006; **281**: 12093-101.

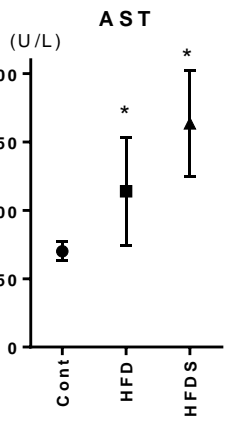
27  
28  
29  
30  
31

Figure 1

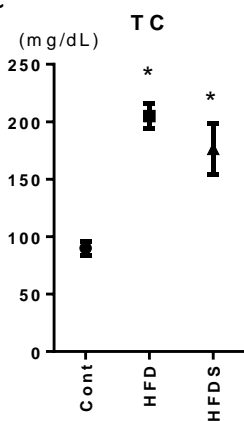
A



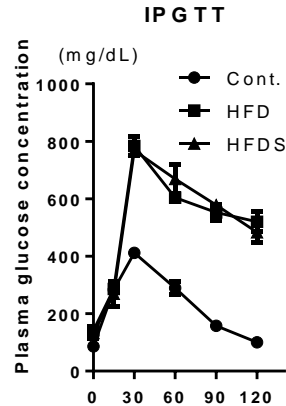
B



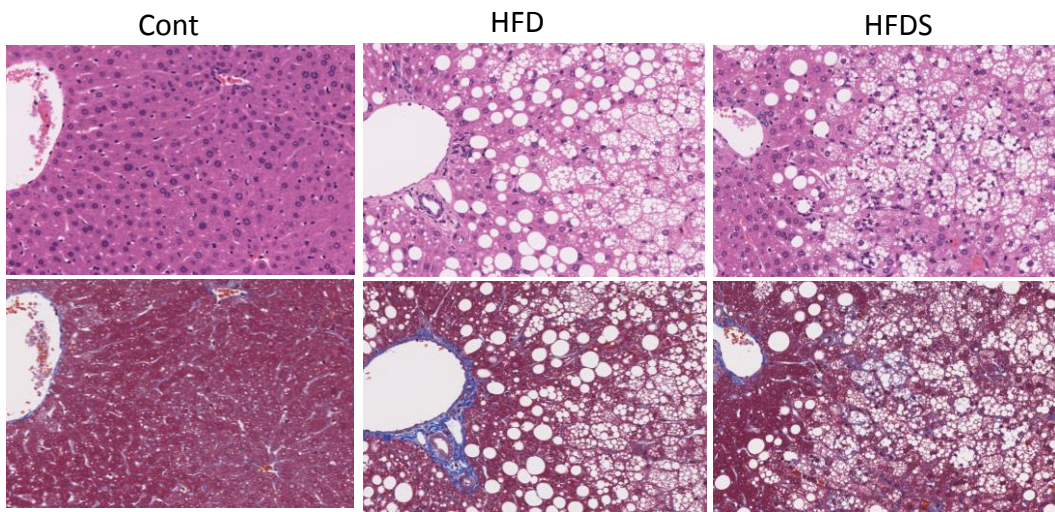
C



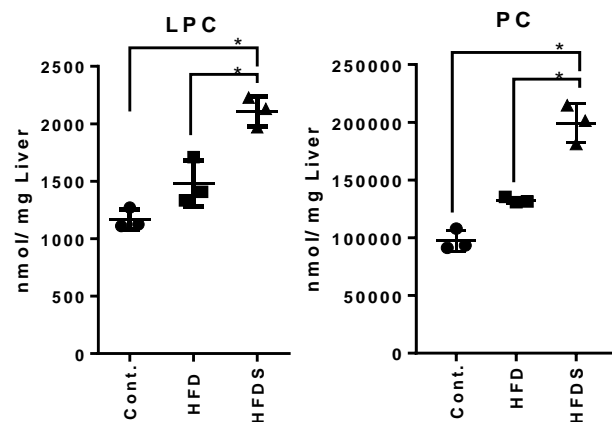
D



E



F



G

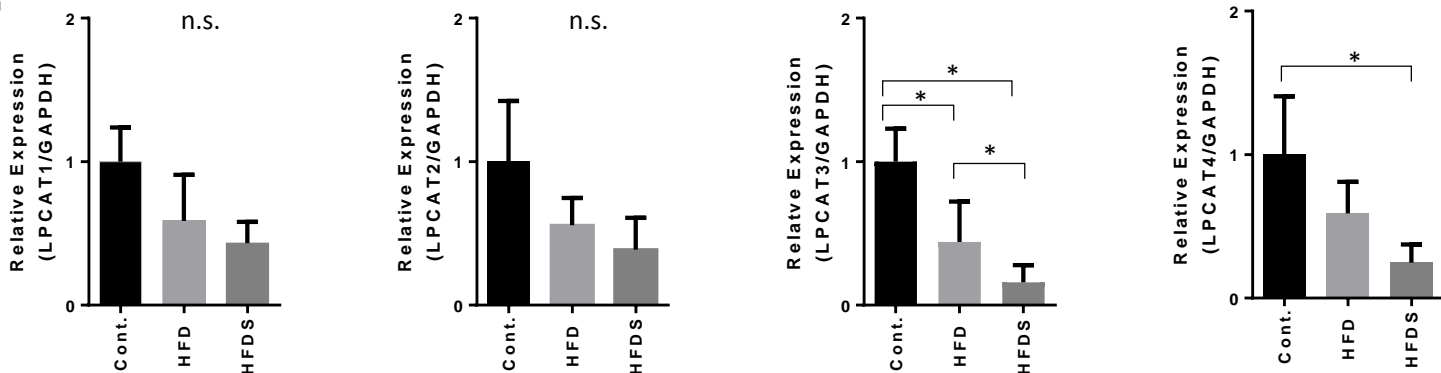


Figure 2

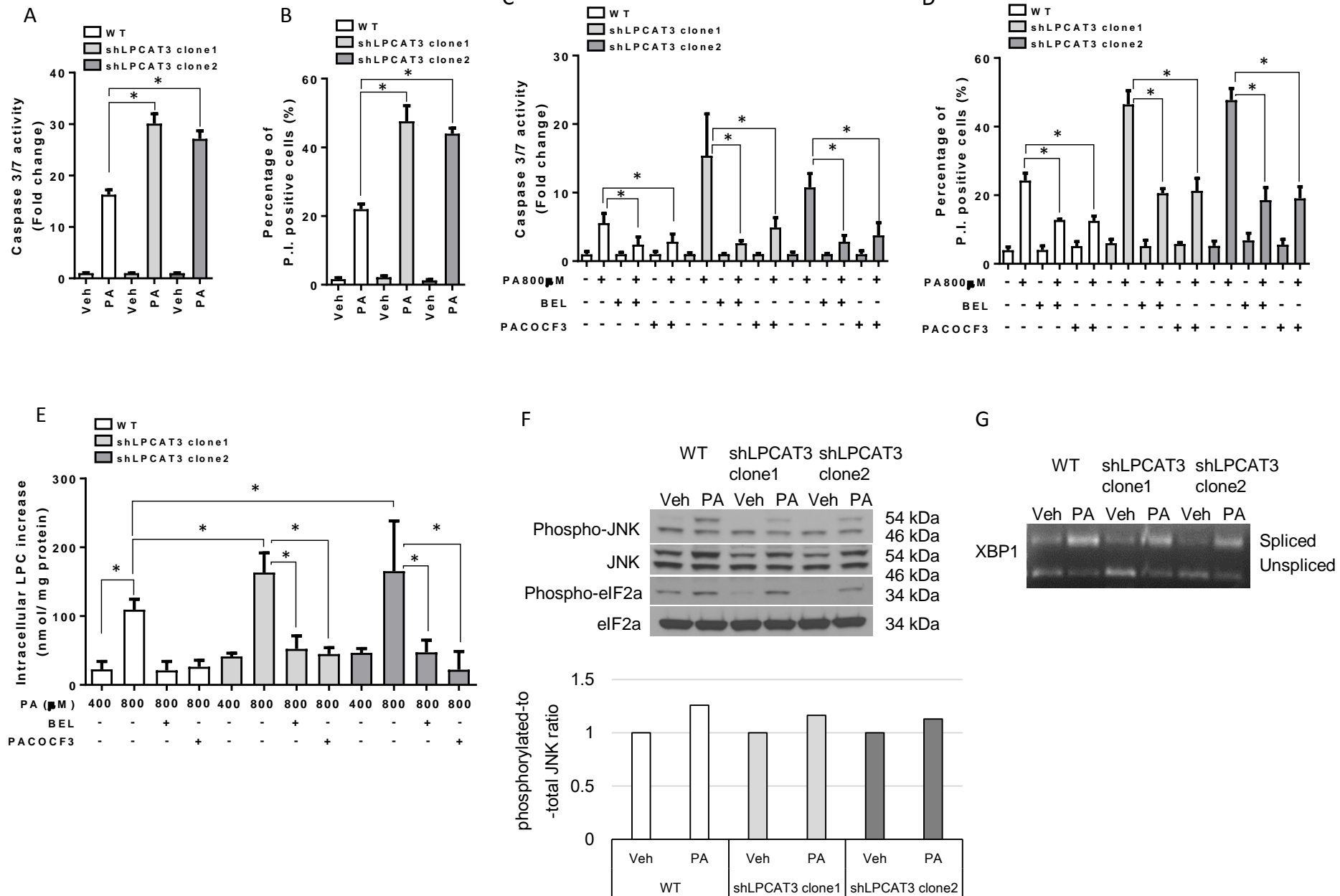


Figure 3

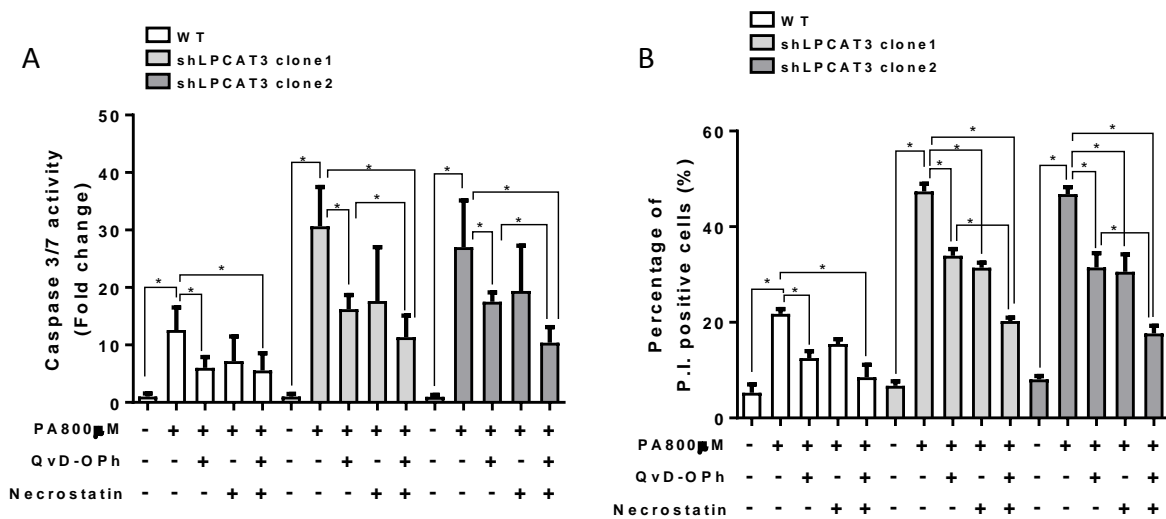
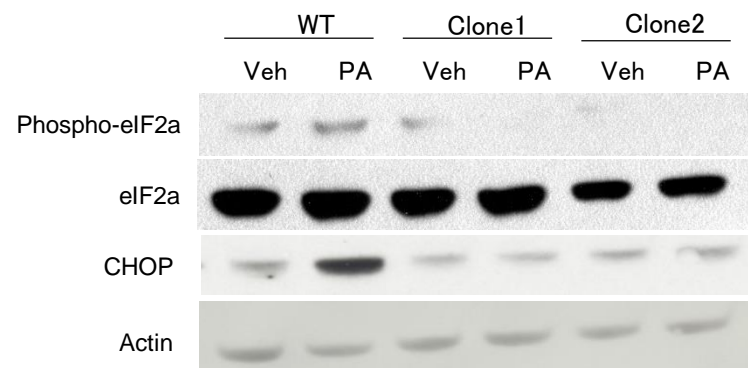
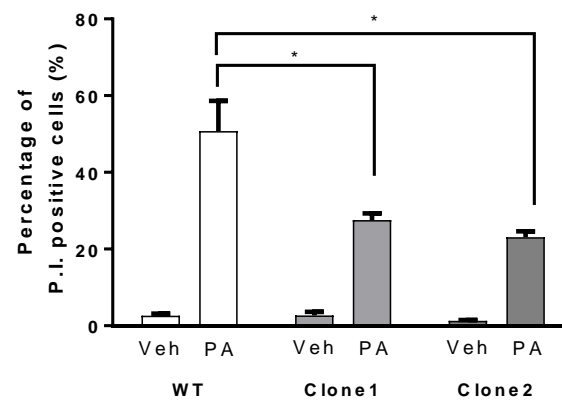


Figure 4

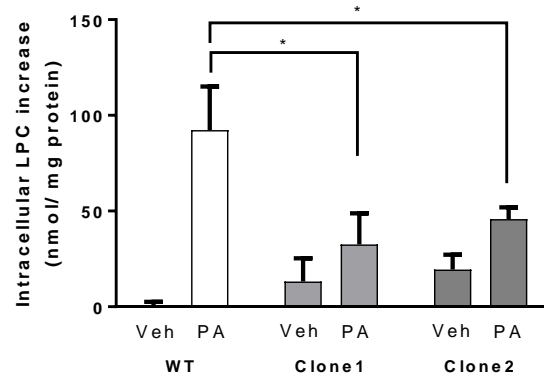
A



B



C



Supplemental material and method

***Intraperitoneal glucose tolerant test.*** The mice were administrated glucose (2 g/kg body weight) intraperitoneally after 6 h of fasting. Blood samples were obtained from the tail vein before glucose administration and at 15, 30, 60, 90, and 120 min after glucose administration.

***Quantitation of cell death.*** Cell death was evaluated by morphological approaches and biochemical methods. For morphological approaches, nuclei were stained by propidium iodide for 30 min at 37 °C and analyzed by fluorescence microscopy (Nikon Eclipse TE200; Nikon, Tokyo, Japan). The number of dead cells was expressed as a percentage of total cells counted. Cell death was also examined by spectrophotometry using Cell Count Reagent SF (Catalog No. 07553; Nakalai Tesque Inc.). The results were presented as the ratio of absorption in the vehicle control group to that in the treatment group. For biochemical methods, we evaluated caspase activity using the Apo-One Caspase-3/7 assay (G7790; Promega, Madison, WI), according to the manufacturer's protocol.

***Quantitative reverse transcription (qRT)-PCR.*** Total cellular RNA was extracted using Trizol reagent (Invitrogen, Camarillo, CA, USA) and was reverse-transcribed into cDNA with Moloney murine leukemia virus reverse transcriptase (Invitrogen,

Camarillo, CA, USA) and random primers (Invitrogen, Camarillo, CA, USA) as previously described <sup>15</sup>. The cDNA was used as a template for qRT-PCR, which was carried out on a LightCycler instrument (Roche Applied Science) using SYBR green (Molecular Probes) as a fluorophore. PCR primers were as follows: for mouse LPCAT1 (NM\_145376.5): forward 5'-ccctgggacctcctgataa-3' and reverse 5'-gcaggaagtccacgacctt-3' (69 bp), for mouse LPCAT2 (NM\_173014.1): forward 5'-tgtactaatcgctcctgtttgatt-3' and reverse 5'-cactggaactcctgggatg-3' (63 bp), for mouse LPCAT3 (NM\_145130.2): forward 5'-ggcctctcaattgcttatttca-3' and reverse 5'-agcacgacacatagcaagga-3' (65 bp), for mouse LPCAT4 (NM\_207206.2): forward 5'-ggcctccagagggttaagtt-3' and reverse 5'-aaaagctagaagtactcggattgg-3' (69 bp), for mouse GAPDH (NM\_001289726.1): forward 5'-gggttctataaatacggactgc-3' and reverse 5'-ccattttgtctacgggacga-3' (112 bp), for human LPCAT3 (NM\_005768.5): forward 5'-accaggaaagatacacaacagc-3' and reverse 5'-ggtagaaaaggcccagactca-3' (65 bp), for human GAPDH (NM\_002046.5): forward 5'-agccacatcgctcagacac-3' and reverse 5'-gcccaatacgaacaaatcc-3' (66 bp). GAPDH was used as an internal control. Gene expression was quantified by the  $2^{-\Delta\Delta CT}$  method, and the target mRNA expression levels were expressed relative to GAPDH per sample as previously described <sup>15</sup>.

***Immunoblot analysis.*** Whole cell lysates were prepared as previously

described <sup>15</sup>. Equal amounts of protein (20 to 80 µg) were resolved by SDS-PAGE on a 12.5–15% acrylamide gel, transferred to a nitrocellulose membrane, and incubated with primary antisera. Membranes were incubated with appropriate horseradish peroxidase-conjugated secondary antibodies (Santa Cruz Biotechnology, Santa Cruz, CA). Bound antibody complexes were visualized using chemiluminescent substrate (ECL; Amersham, Arlington Heights, IL) and exposure to Kodak X-OMAT film (Eastman Kodak, Rochester, NY).

***XBP1 splicing analysis.*** RNA was extracted from shLPCAT3 cells subjected to indicated treatments and transcribed into cDNA. XBP1 was amplified by PCR using forward primer, 5'-AAACAGAGTAGCAGCTCAGACTGC-3', and reverse primer, 5'-TCCTTCTGGGTAGACCTCTGGGAG-3'. The PCR product was digested using the *Pst*I restriction enzyme for 1 h at 37 °C, and then electrophoresed on a 1.7 % agarose gel. The gels were photographed under UV transillumination.

***Antibodies and reagents.*** Antisera used were obtained from the following sources: rabbit anti-phospho-eIF2 $\alpha$  (1:1000; #9721), rabbit anti-eIF2 $\alpha$  (1:1000; #9722), rabbit anti-phospho-JNK (1:1000; #9251), rabbit anti-JNK (1:1000; #9252, Cell Signaling Technology, Danvers, MA, USA); mouse anti-C/EBP homologous protein (CHOP [1:500; sc-575]), and goat anti- $\beta$ -actin (1:1000; sc-1616, Santa Cruz

Biotechnology, Santa Cruz, CA, USA). The pan-caspase inhibitor Q-Val-Asp-Oph (QVD-Oph) was obtained from MP Biomedicals Japan (Tokyo, Japan). The receptor interacting protein 1 kinase (RIPK1) inhibitor was obtained from Selleckchem (Houston, TX, USA). To determine effect of these pharmacological inhibitors to Huh-7 with PA, the cells were incubated with PA (800  $\mu$ M) in the presence of QVD-Oph (20  $\mu$ M) alone, necrostatine (100  $\mu$ M) alone or combination of these agents for 6 h. Bromoenol lactone (BEL; B1552), palmityl trifluoromethyl ketone (PACOCF<sub>3</sub>; P8727), BSA, Bradford reagent, and other chemicals were all obtained from Sigma-Aldrich (St. Louis, MO, USA). To determine effect of each phospholipase A2 inhibitors to Huh-7 with PA, BEL of 20  $\mu$ M or PACOCF<sub>3</sub> of 60  $\mu$ M was incubated with PA for 6 h.

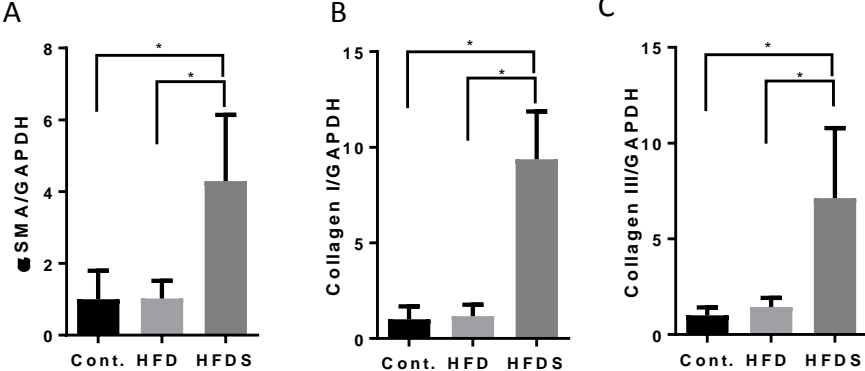
## Supplemental Figure Legends

**Supplemental Figure 1. Expression of genes associated with liver fibrosis in mice fed normal chow, high-fat diet, and high-fat diet with sucrose.** *A, B, and C.* Total RNA was prepared from the livers of mice fed normal chow (Cont), high-fat diet (HFD), or high-fat diet with sucrose (HFDS). mRNA levels of  $\alpha$ SMA (A), collagen I (B), and collagen III (C) were quantified by qRT-PCR, normalized to GAPDH, and expressed as fold change over vehicle. All data are expressed as the mean  $\pm$  SD from four experiments; \* $P$ <0.05.

## **Supplemental Figure 2.**

*A and B,* Total RNA was prepared from Huh-7 cells (WT), LPCAT3 knockdown Huh-7 cells (shLPCAT3), and LPCAT3-overexpressing Huh-7 cells (LPCAT3OE). LPCAT3 expression in shLPCAT3 (A) and LPCAT3OE (B) cells was quantified by qPCR, normalized to GAPDH, and expressed as fold change over WT. All data are expressed as the mean  $\pm$  SD from four experiments; \* $P$ <0.05.

Supplemental Figure 1



Supplemental Figure 2

